Memoirs of the Faculty of Engineering, Kyushu University, Vol.67, No.4, December 2007

Anti-sway Control Input for Overhead Traveling Crane Based on Natural Period

by

Pengfei GAO*, Motoji YAMAMOTO** and Yoshiaki HAYASHI*

(Received November 5, 2007)

Abstract

For safe and efficient work of handling task for heavy load by overhead traveling crane, sway of the suspended load should be avoided. Various methods have been proposed to reduce the sway, mostly by using feedback control methods. However, most material handling system uses open loop type servo controller where trapezoidal or S-shape velocity pattern is typically used for the input of the controller. Considering use of such servo controller, this paper proposes an anti-sway open loop control method based on natural period of the overhead traveling crane system and by using trapezoidal or S-shape velocity pattern for the desired input of the controller. Theoretical analysis for the conditions of no sway by the trapezoidal and S-shape velocity pattern input is presented. This method can be easily applied for an anti-sway control of the crane system when typical servo controller is used. The idea is also applied for the case of changing rope length of the overhead traveling crane system.

Keywords: Overhead traveling crane, Anti-sway control, natural period, Trapezoidal velocity pattern, S-shaped velocity pattern

1. Introduction

Many types of crane mechanisms are widely used for handling heavy load. Especially, traveling crane is generally used such as gantry cranes in port yard and overhead traveling cranes in manufacturing factories. While handling work by the crane mechanism, the load is easy to swing because the load is suspended by single rope. The swing is danger for workers in the workspace of the crane and it lowers the efficiency of the handling work, because it takes time to reduce the swing for positioning of the load. Thus, lots of studies on anti-sway control have been done by many researchers.

To reduce the sway of the suspended load of gantry crane and overhead traveling crane, many linear-feedback control theory based methods have been proposed[1)-4)]. Most of them are combination methods of linear control theory and a compensation control, because the crane system is essentially a nonlinear system. For example, a control method by linear regulator and

* Graduate Student, Department of Intelligent Machinery and Systems
** Professor, Department of Intelligent Machinery and Systems

compensation input for non-linear part[5], a method by multiple optimum regulators' gains for changing rope length[6], a combination method of linear feedback and disturbance observer[7] are proposed.

To deal with the non-linearity of the crane system directly, some non-linear feedback control methods [8)-10)] such as input-output linearization method have been proposed. Furthermore, using the operator's skill for the crane work, fuzzy or rule base feedback control methods[11)-13)] are also proposed for anti-sway of suspended load. These control methods are state feedback type using the state of the load such as swing angle, where some sensor systems to detect the state are needed. That becomes a complicated control system.

On the other hand, trajectory following control by using pre-designed optimum control input can be also applied to the anti-sway control problem. For example, control input design by maximum principle and typical input pattern of less sway are proposed[14)- 17)]. Combination of typical input pattern and linear feedback control are also proposed[18)-20)].

In addition to crane mechanisms, many positioning and servo mechanisms use a servo controller, where desirable velocity and trajectory are realized by an inner feedback loop inside of the controller when suitable desirable control inputs are commanded to the controller. Thus user is just requested to input the desirable values for the controller without feedback of state of mechanism. When such servo controller is installed as a control system, trapezoidal velocity pattern or S-shape velocity pattern are often used as the desirable trajectory of the mechanism. This control is basically an open-loop type in the view point of the user when using the servo controller.

For such case, it has been known by experience that using natural period of the mechanism as the acceleration period of trapezoidal velocity pattern leads to low sway of the system. However, theoretical background and mathematical condition has not been cleared yet. Thus, considering the fact that many servo mechanisms are controlled by trapezoidal velocity pattern or S-shape velocity pattern, the paper proposes a design method of no sway control input for overhead traveling crane system by the typical velocity pattern. This is a method based on the relation between acceleration time of the typical velocity pattern and natural period of the crane system. The paper gives theoretical background for the experimental knowledge of the natural period method, and leads to general conditions for no sway using various velocity input patterns. This paper also makes clear that there is a condition of no sway when S-shape velocity pattern is used. When the rope length is changed during traveling of the trolley, this idea of no sway can not be applied directly, because natural period is continuously changed for the changing rope's length. However, the paper shows that there is no sway if the rope length is changed at constant velocity interval.

The paper, firstly, presents dynamical model of the over head traveling crane system. Then, no sway condition using trapezoidal velocity pattern with and without damping is shown. Furthermore, no sway condition using S-shape velocity pattern with and without damping is also shown. The case of changing rope length is discussed. Validity of the proposed control design method of no sway control input is confirmed by numerical simulations.

2. Dynamical Model of Overhead Traveling Crane

This section shows a dynamical model of overhead traveling crane. For simplicity, it is assumed that suspended load is point mass, mass of rope is small enough comparing the suspended load, the rope does not generate bending moment and the rope does not get longer. Then, the equation of motion of load along constrained arc by rope is

$$m\ddot{s} = -mg\sin\phi + m\ddot{x}\cos\phi \tag{1}$$

where x is trolley position, m is mass of the suspended load, g is gravitational force, ϕ is swing angle of rope and s is the coordinate value along constrained arc by rope (see **Fig.1**).

Setting l as rope length which can change for time t, introducing viscous damping term C and using $s=l\phi$, Equation (1) leads

$$\ddot{\phi}+\left(\frac{C+2\dot{l}}{l}\right)\dot{\phi}+\left(\frac{g+\ddot{l}}{l}\right)\phi=\frac{\ddot{x}}{l} \tag{2}$$

This is a second order time variant system differential equation. If rope length is not changed, the equation becomes

$$\ddot{\phi}+\frac{C}{l}\dot{\phi}+\frac{g}{l}\phi=\frac{\ddot{x}}{l} \tag{3}$$

where the natural period for the system is

$$T_n=2\pi\sqrt{\frac{l}{g}} \tag{4}$$

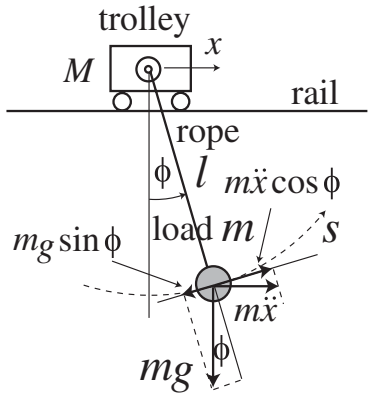

Fig. 1 Model of overhead traveling crane**.**

3. Trapezoidal Velocity Pattern and Natural Period

When using a commercial servo controller, trapezoidal velocity pattern is often used for position control of mechanical systems. It has been known by experience that taking same value for natural period of the mechanism and the acceleration interval of trapezoidal velocity pattern leads to no sway of the system. This section, thus, discusses general relationship between sway of the system and design of trapezoidal velocity pattern. In this section, rope length is assumed to be constant. The case of changing rope length is treated in the later section.

3.1 Case of no damping

This subsection discusses the case where the trolley is controlled by trapezoidal velocity pattern assuming no damping in the crane system. In actual positioning task by overhead traveling crane, the traveling distance L is specified in advance. By the limit of driving system for trolley, maximum velocity of the trolley $v_{\max}$ is also specified. Then the traveling distance L and acceleration and deceleration interval T_1 and constant speed interval T_2 hold the following relation

$$L=v_{\max}(T_1+T_2) \qquad \text{if } \frac{L}{v_{\max}}-T_1\geq 0 \tag{5}$$

Because L and v_{max} is specified, T_2 is automatically determined when T_1 is specified by the condition of no sway.

By assuming no change of rope length, we calculate the response for the trapezoidal velocity input in **Fig.2** from 0 to T_1. Firstly, rewrite the equation (3) by standard form of second order system as

$$\ddot{\phi} + 2\zeta\omega_n\dot{\phi} + \omega_n{}^2\phi = u(t) \tag{6}$$

where ζ ($0 \le \zeta \le 1$; because the typical crane mechanism has very low damping coefficient) is damping coefficient, ω_n is natural angular frequency and $u(t)$ is input for the system. By setting constant input $u(t) = a(0 \le t \le T_1)$, the response is

$$\phi(t) = e^{-\zeta\omega_n t}(C_1 \cos\sqrt{1-\zeta^2}\,\omega_n t + C_2 \sin\sqrt{1-\zeta^2}\,\omega_n t) + \frac{a}{\omega_n{}^2} \tag{7}$$

Using initial condition of $\phi = 0$ and $\dot{\phi} = 0$ at t=0, and assuming no dumping $(\zeta = 0)$,

$$\phi(t) = \frac{a}{\omega_n{}^2}(1 - \cos\omega_n t) \tag{8}$$

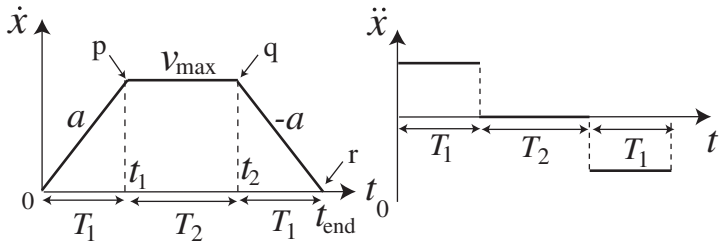

Fig. 2 Trapezoidal velocity pattern.

At the point p in the **Fig.2**, $\phi = 0$ and $\dot{\phi} = 0$ for no sway at $t = T_1$, thus

$$\phi = \frac{a}{\omega_n{}^2}(1 - \cos\omega_n T_1) = 0 \tag{9}$$

$$\dot{\phi} = \frac{a}{\omega_n}\sin\omega_n T_1 = 0 \tag{10}$$

This condition leads to

$$\omega_n T_1 = 2n\pi \quad n = 1,2,\cdots \tag{11}$$

Using the natural period of the system T_n (Equation (4)), the condition is rewritten by

$$T_1 = \frac{2n\pi}{\omega_n} = nT_n \quad n = 1,2,\cdots \tag{12}$$

This condition means that taking same value for the acceleration interval and n times of natural period leads to no sway of the crane system at point p in **Fig.2**. The interval of $t_2 \le t \le t_{end}$ is completely symmetrical with the interval of $0 \le t \le t_1$. Thus there is no sway at $t = t_{end}$ if the

Equation (12) is satisfied. Furthermore, there is no sway during constant speed section $t_1 \le t \le t_2$, because zero input for the Equation (6) and $\phi(t_1) = 0, \dot{\phi}(t_1) = 0$. Note that same *n* for acceleration interval and deceleration interval is not necessary. For example acceleration interval $0 \le t \le t_1$ is $2T_n$ and deceleration interval $t_2 \le t \le t_{end}$ is $3T_n$ will also be no sway at point p, q, r in **Fig.2**.

3.2 Case of with damping

When there is damping effect in dynamical equation (6), the condition of no sway changes. This subsection derives the condition. We first rewrite the Equation (7) using the initial condition $\phi(0) = 0, \dot{\phi}(0) = 0$ as

$$\phi(t) = \frac{a}{{\omega_n}^2}\left[1 - \frac{e^{-\zeta\omega_n t}}{\sqrt{1-\zeta^2}}\sin\left(\omega_n\sqrt{1-\zeta^2}\,t + \tan^{-1}\frac{\sqrt{1-\zeta^2}}{\zeta}\right)\right] \tag{13}$$

By the condition of $\phi(T_1) = 0, \dot{\phi}(T_1) = 0$,

$$\frac{e^{-\zeta\omega_n T_1}}{\sqrt{1-\zeta^2}}\sin\left(\omega_n\sqrt{1-\zeta^2}\,T_1 + \theta(\zeta)\right) = 1 \tag{14}$$

$$\zeta\omega_n\sin\left(\omega_n\sqrt{1-\zeta^2}\,T_1 + \theta(\zeta)\right) - \omega_n\sqrt{1-\zeta^2}\cos\left(\omega_n\sqrt{1-\zeta^2}\,T_1 + \theta(\zeta)\right) = 0 \tag{15}$$

where $\theta(\zeta) = \tan^{-1}\dfrac{\sqrt{1-\zeta^2}}{\zeta}$.

From equation (14) and (15),

$$\cos\left(\omega_n\sqrt{1-\zeta^2}\,T_1 + \theta(\xi)\right) = \zeta e^{\zeta\omega_n T_1} \tag{16}$$

This is a condition of no sway on T_1, however, it is not clear that there is a solution of T_1 or not for the nonlinear equation (16).

3.3 Case of without constant speed interval

This subsection discusses the case of $\dfrac{L}{v_{\max}} - T_1 < 0$. For such case, constant speed interval in **Fig.2** is disappeared, and maximum speed of the trolley does not reach to specified $v_{\max}$ and holds

$$L = aT_1^{\,2} \tag{17}$$

When the T_1 is specified for the condition of no sway, the constant acceleration *a* is automatically determined, because *L* is specified.

The response for the interval $0 \le t \le t_1$ is as same as the one in section **3.2** and **3.3**, because of same terminal conditions and same constant input *a*. Thus the condition of no sway for the case of without damping is

$$T_1 = \frac{2n\pi}{\omega_n} = nT_n \qquad n = 1,2,\cdots \tag{18}$$

And for the case of with damping, no sway condition is the Equation (16).

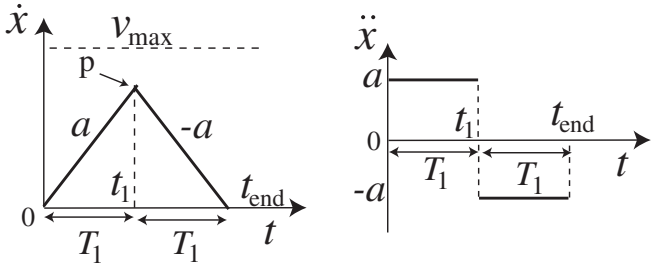

Fig. 3 Trapezoidal velocity pattern without constant speed interval.

4. S-Shape Velocity Pattern and Natural Period

When trapezoidal velocity pattern is used for a positioning control of mechanical systems, undesirable vibration may be excited for the system because of discontinuity for input acceleration at switching points (point p and q in **Fig.2**). Therefore, smoother curve is desirable for the velocity patter. The S-shape velocity pattern is often used as a desirable input for servo controller for such reason. Where the velocity is second order polynomial function on time *t*, which is shown in **Fig.4**. This section discusses a no sway condition using the S-shape velocity pattern.

4.1 Case of no dumping

When the velocity pattern is given in **Fig.4**, the relationship between traveling distance of trolley L and acceleration and deceleration interval T_1 and constant speed interval T_2 is

$$L = v_{\max}(2T_1 + T_2) \qquad \text{if} \quad \frac{L}{v_{\max}} - 2T_1 \geq 0 \tag{19}$$

Where L and $v_{\max}$ is specified in actual positioning problem, thus constant speed interval T_2 is automatically determined if the interval of T_1 is given by the following no sway condition. The slope a of input $u(t)$ in **Fig.4** is given by

$$a = \frac{v_{\max}}{T_1^{\,2}} \tag{20}$$

Thus, for given $v_{\max,}$ the slope a is automatically determined by calculating T_1 by the following no sway condition.

For the dynamical system equation (6), response of sway angle $\phi(t)$ for the S-shape velocity pattern is expressed by the form of

$$\phi(t) = e^{-\zeta\omega_n t}\left(C_1 \cos\sqrt{1-\zeta^2}\,\omega_n t + C_2 \sin\sqrt{1-\zeta^2}\,\omega_n t\right) + (At + B) \tag{21}$$

where C_1, C_2, A, B are constants determined by initial condition and input. Assuming no dumping, the response with zero initial condition, the sway angle and velocity of sway angle for the interval $0 \leq t \leq T_1$ are

$$\phi(t) = -\frac{a}{\omega_n{}^3}\sin\omega_n t + \frac{at}{\omega_n{}^2} \tag{22}$$

$$\dot{\phi}(t) = -\frac{a}{\omega_n{}^2}\cos\omega_n t + \frac{a}{\omega_n{}^2} \tag{23}$$

Using terminal condition in the Equations (22), (23), for the interval $T_1 \le t \le 2T_1$,

$$\phi(t) = \frac{2aT_1}{\omega_n{}^2}\cos\omega_n t + \frac{a}{\omega_n{}^3}\sin\omega_n t - \frac{at}{\omega_n{}^2} \tag{24}$$

$$\dot{\phi}(t) = -\frac{2aT_1}{\omega_n}\sin\omega_n t + \frac{a}{\omega_n{}^2}\cos\omega_n t - \frac{a}{\omega_n{}^2} \tag{25}$$

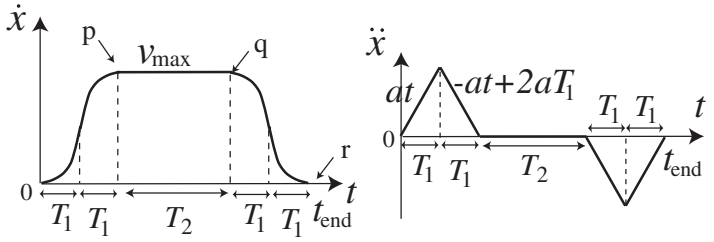

Fig. 4 S-shape velocity pattern.

No sway condition at time $t = 2T_1$ is given by the Equations (24), (25) as;

$$\phi = \frac{2aT_1}{\omega_n{}^2}\cos\omega_n 2T_1 + \frac{a}{\omega_n{}^3}\sin\omega_n 2T_1 - \frac{2aT_1}{\omega_n{}^2} = 0 \tag{26}$$

$$\dot{\phi} = -\frac{2aT_1}{\omega_n}\sin\omega_n 2T_1 + \frac{a}{\omega_n{}^2}\cos\omega_n 2T_1 - \frac{a}{\omega_n{}^2} = 0 \tag{27}$$

Therefore the condition of no sway at p, q, r in **Fig.4** with S-shape velocity pattern is

$$T_1 = \frac{2n\pi}{\omega_n} = nT_n \qquad (n = 1,2,\cdots) \tag{28}$$

4.2 Case of with dumping

The condition of no sway for the case of considering dumping is discussed. Based on the dynamics equation (6), sway angle ϕ (t) is described using the S-shape velocity input in **Fig.4** as,

$$\phi(t) = e^{-\zeta\omega_n t}\left(C_1\cos\sqrt{1-\zeta^2}\,\omega_n t + C_2\sin\sqrt{1-\zeta^2}\,\omega_n t\right) + (At + B) \tag{29}$$

where, $C_1 = \frac{-2\varsigma a}{\omega_n{}^3}$ $C_2 = \frac{a(1-2\varsigma^2)}{\omega_n{}^3\sqrt{1-\varsigma^2}}$ $A = -\frac{a}{\omega_n{}^2}$ $B = \frac{2\varsigma a}{\omega_n{}^3}$

The sway angle response for the interval $0 \le t \le T_1$ is

$$\phi(t) = e^{-\varsigma\omega_n t}\left(\frac{-2\varsigma a}{\omega_n{}^3}\cos(\sqrt{1-\varsigma^2}\,\omega_n t) + \frac{a(1-2\varsigma^2)}{\omega_n{}^3\sqrt{1-\varsigma^2}}\sin(\sqrt{1-\varsigma^2}\,\omega_n t)\right) - \left(\frac{a}{\omega_n{}^2}t - \frac{2\varsigma a}{\omega_n{}^3}\right) \tag{30}$$

$$\dot{\phi} = e^{-\varsigma\omega_n t}\left(\frac{a}{\omega_n{}^2}\cos(\sqrt{1-\varsigma^2}\,\omega_n t) + \frac{\varsigma a}{\omega_n{}^2\sqrt{1-\varsigma^2}}\sin(\sqrt{1-\varsigma^2}\,\omega_n t)\right) - \frac{a}{\omega_n{}^2} \tag{31}$$

For the interval $T_1 \le t \le 2T_1$, ϕ (t) is given by equation (29) where

$$C_1 = \frac{-2\zeta a}{\omega_n{}^3} - \frac{2e^{\zeta\omega_n T_1}}{\cos\sqrt{1-\varsigma^2}\,\omega_n T_1}\left(\frac{aT_1}{\omega_n{}^2} - \frac{2\varsigma a}{\omega_n{}^3}\right) \tag{32}$$
$$+ 2e^{\zeta\omega_n T_1}\frac{\tan(\sqrt{1-\varsigma^2}\,\omega_n T_1)}{\omega_n\sqrt{1-\zeta^2}}\frac{\frac{a}{\omega_n{}^2} + (\frac{aT_1}{\omega_n} - \frac{2\zeta a}{\omega_n{}^2})(\zeta + \sqrt{1-\varsigma^2}\tan(\sqrt{1-\varsigma^2}\,\omega_n T_1))}{\cos(\sqrt{1-\varsigma^2}\,\omega_n T_1) + \sin(\sqrt{1-\varsigma^2}\,\omega_n T_1)\tan(\sqrt{1-\varsigma^2}\,\omega_n T_1)}$$

$$C_2 = \frac{a(1-\zeta)}{\omega_n{}^3\sqrt{1-\varsigma^2}} - \frac{2e^{\zeta\omega_n T_1}}{\omega_n\sqrt{1-\zeta^2}}\left[\frac{\frac{a}{\omega_n{}^2} + (\frac{aT_1}{\omega_n} - \frac{2\zeta a}{\omega_n{}^2})(\zeta + \sqrt{1-\varsigma^2}\tan(\sqrt{1-\varsigma^2}\,\omega_n T_1))}{\cos\sqrt{1-\varsigma^2}\,\omega_n T_1 + \sin(\sqrt{1-\varsigma^2}\,\omega_n T_1)\tan(\sqrt{1-\varsigma^2}\,\omega_n T_1)}\right] \tag{33}$$

$$A = \frac{a}{\omega_n{}^2} \qquad B = -\frac{2\varsigma a}{\omega_n{}^3} \tag{34}$$

$\dot{\phi}(t)$ $(T_1 \le t \le 2T_1)$ is given by equation (29) where

$$C_1 = \frac{a}{\omega_n{}^2} - \frac{2\zeta e^{\zeta\omega_n T_1}}{\cos\sqrt{1-\varsigma^2}\,\omega_n T_1}\left(\frac{aT_1}{\omega_n} - \frac{2\varsigma a}{\omega_n{}^2}\right) \tag{35}$$
$$- 2e^{\zeta\omega_n T_1}(1 + \frac{\zeta}{\sqrt{1-\varsigma^2}}\tan(\sqrt{1-\varsigma^2}\,\omega_n T_1))\frac{\frac{a}{\omega_n{}^2} + (\frac{aT_1}{\omega_n} - \frac{2\zeta a}{\omega_n{}^2})(\zeta + \sqrt{1-\varsigma^2}\tan(\sqrt{1-\varsigma^2}\,\omega_n T_1))}{\cos(\sqrt{1-\varsigma^2}\,\omega_n T_1) + \sin(\sqrt{1-\varsigma^2}\,\omega_n T_1)\tan(\sqrt{1-\varsigma^2}\,\omega_n T_1)}$$

$$C_2 = \frac{a\zeta}{\omega_n{}^2\sqrt{1-\varsigma^2}} + \frac{2e^{\zeta\omega_n T_1}\sqrt{1-\zeta^2}}{\cos\sqrt{1-\varsigma^2}\,\omega_n T}(\frac{aT_1}{\omega_n} - \frac{2a\zeta}{\omega_n{}^2}) \tag{36}$$
$$+ 2e^{\zeta\omega_n T_1}(\frac{\zeta}{\sqrt{1-\zeta^2}} - \tan(\sqrt{1-\varsigma^2}\,\omega_n T))\left[\frac{\frac{a}{\omega_n{}^2} + (\frac{aT_1}{\omega_n} - \frac{2\zeta a}{\omega_n{}^2})(\zeta - \sqrt{1-\varsigma^2}\tan(\sqrt{1-\varsigma^2}\,\omega_n T_1))}{\cos\sqrt{1-\varsigma^2}\,\omega_n T_1 + \sin(\sqrt{1-\varsigma^2}\,\omega_n T_1)\tan(\sqrt{1-\varsigma^2}\,\omega_n T_1)}\right]$$

$$A = 0 \qquad B = \frac{a}{\omega_n{}^2} \tag{37}$$

Then no sway condition is obtained by setting $t = 2T_1$ and by setting $\phi(t) = 0$, $\dot{\phi}(t) = 0$ for the above equations. However, the relation is too complicated to get closed form condition for T_1. It is not clear that there is a condition of no sway for the dumping case or not.

4.3 Case of no constant speed interval

When $\frac{L}{v_{\max}} - 2T_1 < 0$, the constant speed interval is disappeared as in **Fig.5**. Then the relationship between the traveling distance of trolley L and T_1 in **Fig.5** is

$$L = 2aT_1^2 \tag{38}$$

The interval of T_1 is given by the following no sway condition, thus the parameter a is determined by the above equation. Then the condition of no sway for T_1 is same as the Equation (28) for no dumping case, and same as the Equations (29), (32)-(37) for dumping case, because of the same condition for $0 \le t < 2T_1$ in section 4.1.

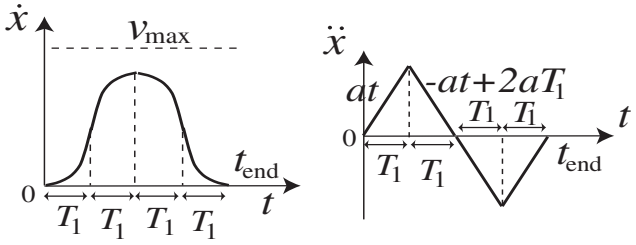

Fig. 5 S-shape velocity pattern without constant speed interval.

5. Numerical Simulation

To confirm a validity of the proposed control input design method for overhead traveling crane for anti-sway control, numerical simulations are presented in this section. In the following simulation, the traveling distance for trolley is L=50[m], mass of the suspended load m=2370[Kg], initial rope length l_0 =15[m], maximum velocity of trolley $v_{\max}$=6.0[m/sec] for trapezoidal velocity pattern and $v_{\max}$=9.0[m/sec] for S-shape velocity pattern. The natural period T_n =1.2617[sec] for initial rope length.

First simulation example is the case of using trapezoidal velocity pattern as the input of crane system. Figure (T-1) in **Fig.6** is a trapezoidal velocity input with setting the acceleration and deceleration interval T_1 as same value as natural period T_n . Then the response of sway ((T-2) in **Fig.6**) is zero at terminal time. The zero sway is also achieved by setting $T_1 = 2T_n$ as shown in (T-3) and (T-4) in the figures. However, it is found that setting $T_1 = 2.0$ [sec] which is different from n times of natural period ((T-5) and ((T-6) in **Fig.6**) results in residual sway.

Second simulation is the case of using S-shape velocity pattern as the input of crane system. Figure (S-1) and (S-3) in **Fig.7** is the case of proposed velocity input design by S-shape velocity pattern. The figure of (S-5) is not considered on the natural period when determining acceleration and deceleration interval T_1. As shown in (S-2), (S-4) and (S-6) in **Fig.7**, proposed input design method results in no sway at terminal also for the case of S-shape velocity pattern.

Third simulation is the case of changing rope length in **Fig. 8**. In the figure (SR-1), rope length trajectory is given by $l(t)$. Because changing rope length is only in the interval of constant velocity which means zero input, there is no residual sway for this case.

Figures (SC-1), (SC-2), (SC-3) and (SC-4) show the case of considering dumping coefficient C in the Equation (3) where the rope length is fixed with initial value l_0. By setting C=0.2 with trapezoidal velocity pattern and setting T_1=T_n, it is found that a little sway at constant velocity interval and terminal time. This is caused by change of natural period and different phase angle in

Equation (14), (15) from the case of no dumping for sway angle and velocity of sway angle.

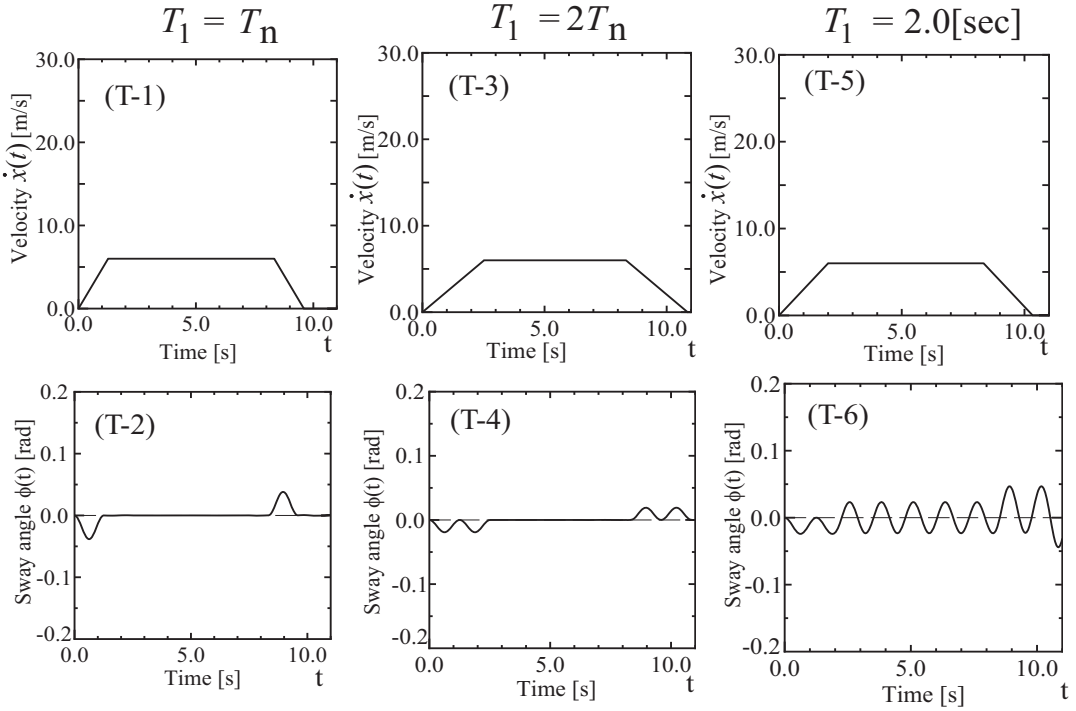

Fig. 6 Trapezoidal velocity pattern by proposed input design method and its response.

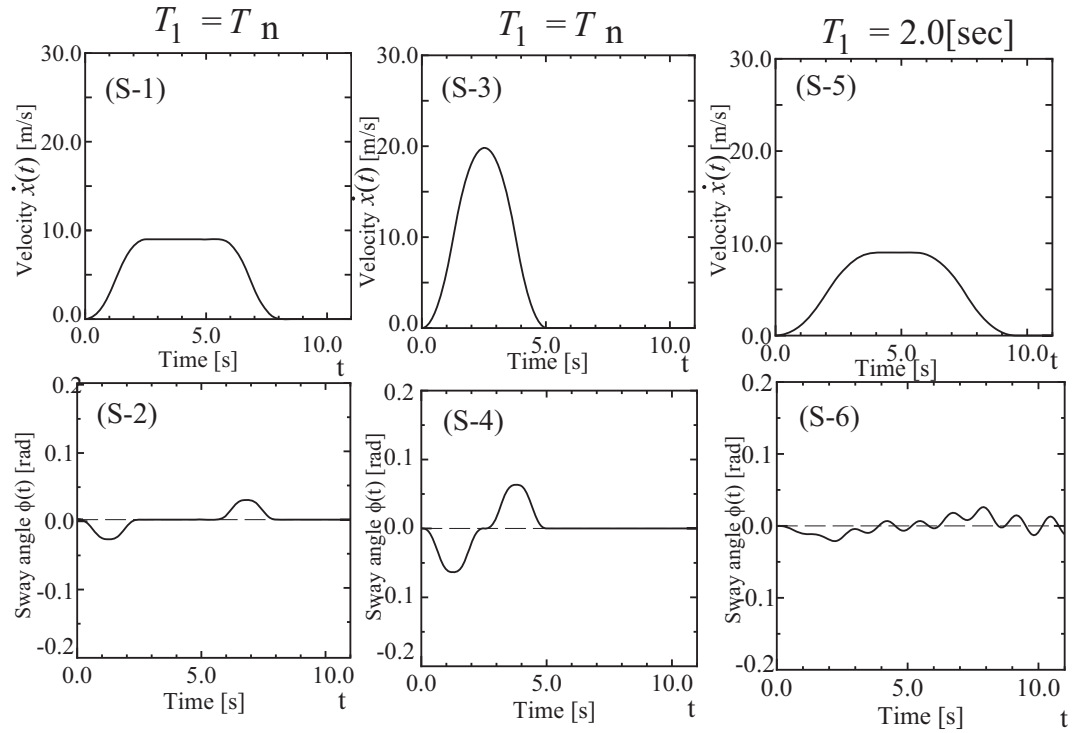

Fig. 7 S-shape velocity pattern by proposed input design method and its response.

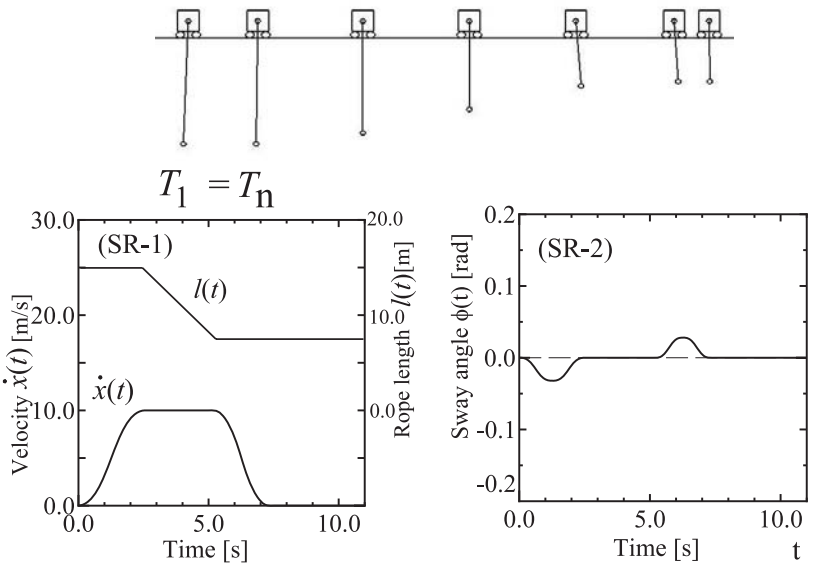

Fig. 8 Case of changing rope length.

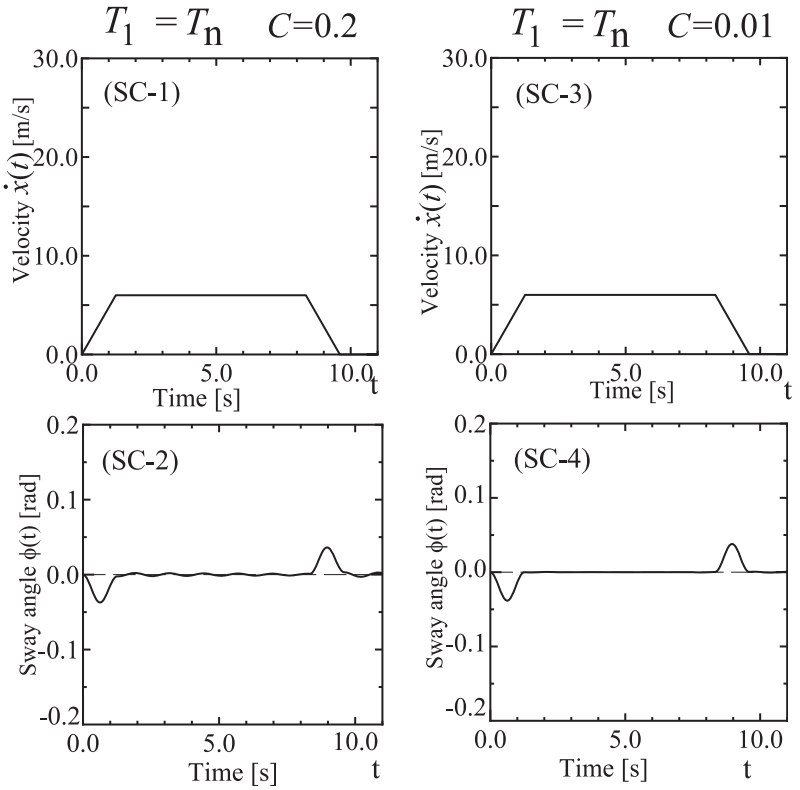

Fig. 9 Case of considering dumping.

However the case of small dumping coefficient C=0.01 which is more practical for typical crane system, little residual sway is found.

6. Conclusion

A control input design for anti-sway of overhead traveling crane based on natural period has been proposed. The paper has discussed the relationship between sway of the suspended load and the natural period of the crane system. We propose an input design method where the acceleration and deceleration interval is set with *n* times of natural period of the crane system when trapezoidal or S- shape velocity input is used. It is also presented that the method can be applied for changing rope length during the motion of trolley if the change of rope is controlled during constant velocity interval both for trapezoidal and S-shape velocity input. Numerical examples show a validity of the proposed anti-sway method.

References

1) K. Tamura, S. Tsunekawa and M. Kobayashi; Control of an Overhead Traveling Crane System with Winding Mechanism and the Application of Adaptive Identification, Transactions on Japan Society of Mechanical Engineers, Series-C Vol.54, No.504, pp.1795-1803 (1988), [in Japanese].
2) K-S. Hong, J-H. Kim and K-I. Lee; Control of a Container Crane: Fast Traversing, and Residual Sway Control from the Perspective of Controlling an Under actuated System, Proc. of the American Control Conference, pp.1294-1298 (1998).
3) N. Kodani, et. al.; An Anti-Sway Control of a Traveling Crane Based on Hoo Control Theory, Proc. of the Annual Conference on System Integration Division of SICE, pp.145-146 (2001), [in Japanese].
4) Y. Hashimoto, et. al.; Load-Swing Suppression Control for Cranes without Oscillation Feedback, Transactions of the Society of Instrument and Control Engineers, Vol.30, No.2, pp.172-180 (1994), [in Japanese].
5) T. Totani, K. Nonami and H. Okamura; A Method for Realizing Linear Optimal Control by Time-Invariant Control Law and Compensation Input, Transactions of the Society of Instrument and Control Engineers, Vol.20, No.3,pp.187-192 (1984), [in Japanese].
6) I. Murata, et. al.; Servo-type Anti-sway Control of Cranes with a Trolley, Transactions on Japan Society of Mechanical Engineers, Series-C Vol.61, No.582, pp.513-518 (1995), [in Japanese].
7) H. Aschemann, et. al.; Disturbance Estimation and Compensation for Trajectory Control of an Overhead Crane, Proc. of the American Control Conference, pp.1027-1031 (2000).
8) N. Yanai, M. Yamamoto and A. Mohri; Feedback Control of Crane Based on Inverse Dynamics Calculation, Transactions of the Society of Instrument and Control Engineers, Vol.37, No.11, pp.1048-1055 (2001), [in Japanese].
9) M. Kobayashi and K. Tamura; Nonlinear Control of Overhead Traveling Crane with Winding Mechanism, Transactions on Japan Society of Mechanical Engineers, Series-C Vol.58, No.584, pp.1318-1326 (1992), [in Japanese].
10) B. Vikramaditya and R. Rajamani; Nonlinear Control of a Trolley Crane System, Proc. of the American Control Conference, pp.1032-1036 (2000).
11) D-Y. Ha; Design of Container Crane Controller Using Intelligence Algorithm, Proc. of the IEEE International Fuzzy Systems Conference, pp.1507-1510 (2001).
12) M. Sakumoto and T. Hayashi; Application of Fuzzy Control to Anti-Sway-System of Container Crane, Transactions on Japan Society of Mechanical Engineers, Series-C Vol.58, No.550,

pp.1792-1797 (1992), [in Japanese].
13) M. Arao, Y. Saito and S. Kawaji; Swing Damping Control using FIMC for Celing-Crane, Proc. of the Annuals Conference on Robotic and Mechatronics Division of Society of Mechanical Engineers, pp.2A1-G8 (2001), [in Japanese].
14) J. Shirai, et. al.; Development of Electronic Sway Control System for Container Crane, Transactions on Japan Society of Mechanical Engineers, Series-C Vol.59, No.561, pp.1443-1447 (1993), [in Japanese].
15) N. Ohira and T. Hisamura; Control of Simple Pendulum with Variable Rope Length, Transactions of the Society of Instrument and Control Engineers, Vol.19, No.9, pp.1759-1761 (1983), [in Japanese].
16) T. Yamagishi; Sway Control for Crane, Proc. of the Joint Conference on Automatic Control, pp.353-354 (1972), [in Japanese].
17) Z. N. Masoud and M. F. Daqaq; A Graphical Approach to Input-Shaping Control Design for Container Cranes With Hoist, IEEE Trans. on Control System Technology, Vol.14, No.6, pp.1070-1077 (2006).
18) Y. Iijima, T. Okawa and O Yamaguchi; Anti-swing Control System for Container Handling Crane, Proc. of the Annual Conference on System Integration Division of SICE, pp.45-46 (2001), [in Japanese].
19) I. Morishita; A New Control Algorithm for the Grab-Swing Elimination in the Automatic Operation of Traveling Cranes, Transactions of the Society of Instrument and Control Engineers, Vol.14, No.6, pp.739-744 (1977), [in Japanese].
20) T. Yamamoto and N. Nomose; A Swing Pendulum Control of the Trolley Crane with Variable Rope Length, Transactions on Japan Society of Mechanical Engineers, Series-C Vol.65, No.633, pp.1787-1794 (1995), [in Japanese].